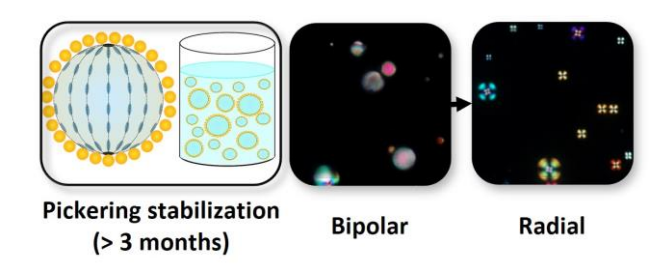
Environmentally Responsive Emulsions of Thermotropic Liquid Crystals with Exceptional Long-Term Stability and Enhanced Sensitivity to Aqueous Amphiphiles

Oscar H. Piñeres-Quiñones, David M. Lynn, 2,3,* and Claribel Acevedo-Vélez^{1,*}

¹Department of Chemical Engineering, University of Puerto Rico-Mayagüez, Call Box 9000, Mayagüez, PR 00681-9000; ²Department of Chemical and Biological Engineering, 1415 Engineering Drive, University of Wisconsin-Madison, Madison, WI 53706, USA; ³Department of Chemistry, University of Wisconsin-Madison, 1101 University Ave., Madison, WI 53706, USA; Email: (D.M.L.) dlynn@engr.wisc.edu; (C.A.V.) claribel.acevedo@upr.edu

ABSTRACT: We report colloidally stable emulsions of thermotropic liquid crystals (LCs) that can detect the presence of amphiphilic analytes in aqueous environments. Our approach makes use of a Pickering stabilization strategy consisting of surfactant-nanoparticle complexes $(SiO_2/C_nTAB, n = 8, 12, 16)$ that adsorb to aqueous/LC droplet interfaces. This strategy can stabilize LC emulsions against coalescence for at least three months. These stabilized LC emulsions also retain the ability to respond to the presence of model anionic, cationic, and nonionic amphiphiles (e.g., SDS, C₁₂TAB, C₁₂E₄) in aqueous solutions by undergoing "bipolarto-radial" changes in LC droplet configurations that can be readily observed and quantified using polarized light microscopy. Our results reveal these ordering transitions to depend upon the length of the hydrocarbon tail of the C_nTAB surfactant used to form the stabilizing complexes. In general, increasing C_nTAB surfactant tail length leads to droplets that respond at lower analyte concentrations, demonstrating that this Pickering stabilization strategy can be used to tune the sensitivities of the stabilized LC droplets. Finally, we demonstrate that these colloidally stable LC droplets can report the presence of rhamnolipid, a biosurfactant produced by the bacterial pathogen Pseudomonas aeruginosa. Overall, our results demonstrate that this Pickering stabilization strategy provides a useful tool for the design of LC droplet-based sensors with substantially improved colloidal stability and new strategies to tune their sensitivities. These advances could increase the potential practical utility of these responsive soft materials as platforms for the detection and reporting of chemical and biological analytes.

For Table of Contents Use Only:



Introduction

Interactions between amphiphilic molecules and thermotropic liquid crystals (LCs) hosted at aqueous interfaces can promote changes in the orientation of the LCs that translate, in many cases, to optical responses that can be readily observed or reported using optical methods (e.g., using polarized light or light scattering). 1-10 The range of molecules that can promote changes in LC orientation in this way is broad, 11-28 and extends from synthetic surfactants 11,12,14,17 to more complex components of biological systems, including lipids, 2,12,24 proteins, 15,19,28 bacterial toxins, 3,22 cells, 16,23 and viruses. 16 Aqueous/LC interfaces thus provide a practical basis for the development of platforms for chemical and biomolecular sensing. Past studies have reported that micrometer-scale droplets of LC dispersed in aqueous phases (e.g., LC-in-water emulsions)²⁹⁻³⁶ provide a versatile approach for designing droplet-based sensors that can respond sensitively to the presence of a wide range of amphiphiles in aqueous environments.^{3,22,36-39} These LC emulsions are straightforward to prepare and deploy and they enable real-time, label-free detection of toxins and other analytes with sensitivities that depend, in general, upon the concentration and structure of the analyte. As one important example, past studies demonstrate that LC emulsions can detect and report the presence of lipid A, a component of bacterial endotoxins, at concentrations as low as 1 pg/mL in water.^{3,22}

While these and other past studies reveal the remarkable sensitivity of LC-in-water emulsions, the practical utility and applied potential of these liquid droplets remains limited by the fact that bare LC droplets are not colloidally stable. These droplets typically aggregate, coalesce, or wet adjacent surfaces over short time periods (e.g., on scales of minutes to hours; Figure 1A), which creates technical challenges associated with accuracy and predictability of response over time, as well as issues associated with preparation and storage for potential

practical applications. Recent studies have addressed issues related to the poor colloidal stability of LC emulsions by coating LC droplets with amphiphilic polymers or polymer-based multilayers that can prevent droplet coalescence (Figure 1B). 31,40-47 These methods can prevent the coalescence of individual droplets, but they can also be compositionally complex and they introduce barriers through which analytes must diffuse to reach the LC interface, both of which can influence the timing and/or sensitivity of response.

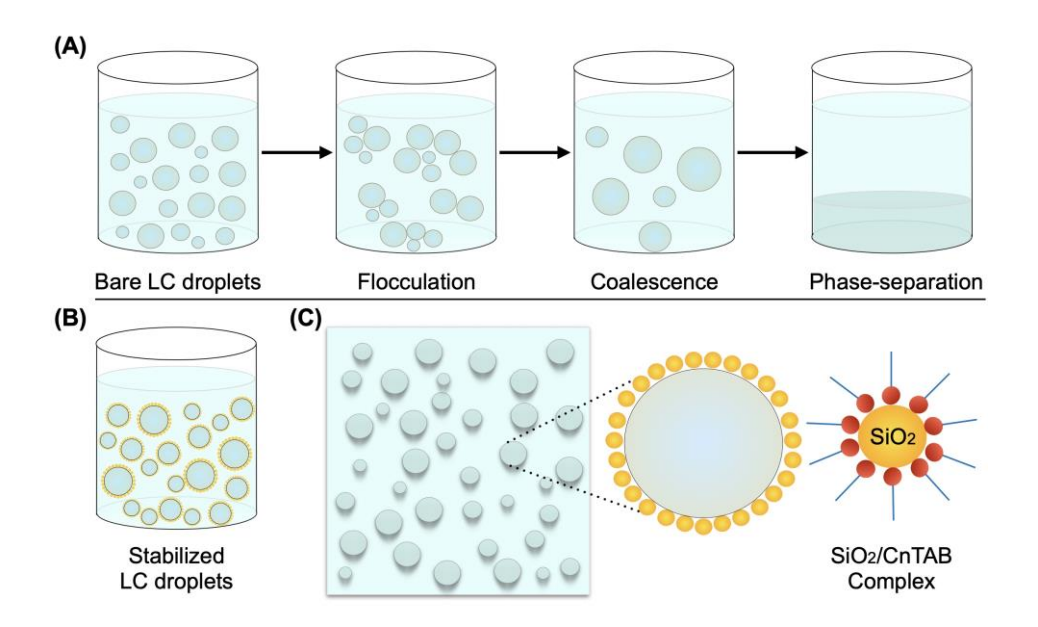


Figure 1. Schematic illustrations of (A) the mechanisms by which bare LC droplets become unstable, (B) colloidally stable LC emulsions, where LC droplets are coated and protected against coalescence, and (C) Pickering LC emulsions stabilized by nanoparticle-surfactant complexes (SiO_2/C_nTAB , n = 8, 12, 16).

The work reported here was motivated broadly by strategies for the stabilization of oil droplets using so-called "Pickering emulsions" created by the adsorption of nanoparticles to the oil/water interfaces of droplets suspended in aqueous environments (e.g., Figure 1C).⁴⁸⁻⁵⁴ We hypothesized that this approach could be used to both (i) provide colloidal stability to LC emulsion droplets and (ii) provide a means of influencing or fine-tuning the orientational

responses, or other behaviors, of LC droplets in aqueous environments (e.g., by varying the size or surface composition of the adsorbed nanoparticles, etc.). During the course of our studies, Dan et al.³⁸ reported that the adsorption of whey protein microgel particles to aqueous/LC interfaces could stabilize LC droplet emulsions for up to 14 days, and that these stabilized droplets permit the transport of synthetic amphiphiles such as sodium dodecyl sulfate (SDS) to the LC-water interface to trigger ordering transitions. That work provides exciting support for the potential roles that Pickering emulsions can play in stabilizing responsive LC droplet sensors. However, the concentrations of SDS required to induce an LC response in that study were reported to be higher than those required to induce transitions in bare LC droplets, suggesting that the properties of the stabilizing protein microgel particles used in that study also influence (and, in some cases, diminish) droplet sensitivity. Here, we report new designs of nanoparticle-based Pickering-type LC emulsions that exhibit both significantly enhanced colloidal stability and improved sensitivity toward aqueous amphiphiles.

Our approach makes use of inorganic nanoparticle/surfactant complexes to prepare Pickering emulsions of the nematic LC 4-cyano-4'-pentylbiphenyl (5CB) in water (Figure 1C). These complexes comprised of silica (SiO₂)nanoparticles are and cationic trimethylalkylammonium bromide surfactants (C_nTAB, n = 8, 12, 16) that have been shown in past studies to accumulate at air-water and oil-water interfaces and stabilize foams and emulsions for extended periods. 49,52,55-57 Our results show that SiO₂/C_nTAB complexes adsorb to LC droplet interfaces and stabilize LC emulsions against coalescence for at least three months. Stabilized droplets that sediment over this time period can be readily re-dispersed by gentle shaking, demonstrating the robust colloidal stability of this system; in contrast, bare LC droplets flocculate and coalesce within hours of preparation, leading to bulk phase separation.

These nanoparticle-stabilized emulsions also respond upon exposure to model anionic, cationic, and nonionic amphiphiles (Figure 2) by undergoing diagnostic "bipolar-to-radial" transitions that can be readily observed using polarized light microscopy. Our results reveal that the bulk concentration of each amphiphile required to trigger these LC ordering transitions depends upon the hydrocarbon tail length of the C_nTAB surfactant used to form the SiO₂/C_nTAB stabilizing complex. In general, increasing the C_nTAB surfactant tail length leads to droplets that respond at lower analyte concentrations, suggesting that this approach can be used to tune the sensitivities of these stabilized LC droplets. LC emulsions stabilized by SiO₂/C₁₆TAB, in particular, respond to SDS at concentrations in the micromolar range (5 μM) that are orders of magnitude lower than those required to trigger similar responses in bare LC droplets (e.g., 0.3

$$C \equiv N$$
 $C \equiv N$
 $C = N$
 C

Figure 2. Chemical structures of the nematic liquid crystal 5CB and the amphiphilic analytes used in this study.

mM), providing further support for this view. These droplets also respond to concentrations of cationic and nonionic surfactants that are significantly higher than those required using anionic SDS, hinting at strategies that could also be used to impart some degree of selectivity using this approach. Finally, we demonstrate that these stabilized LC droplets can be used to report the presence of rhamnolipid (Figure 2), a biosurfactant produced as a virulence factor by the bacterial pathogen *Pseudomonas aeruginosa*, ^{36,58} at biologically relevant concentrations. When combined, our results reveal Pickering LC emulsions stabilized by SiO₂/C_nTAB complexes to provide new and useful approaches for the design of LC droplet-based sensors with substantially improved colloidal stability, as well as guidance that could prove useful for enhancing or tuning the sensitivities and selectivity and, thus, also the practical utility, of these responsive soft materials as platforms for the detection of chemical and biological analytes.

Materials and Methods

Materials. The aqueous silica dispersion Ludox TMA (34 wt.% suspension in H₂O, surface area of ~140 m² g⁻¹, pH of 7, density of 1.23 g cm⁻³at 25 °C, molecular weight of 60.08 g mol⁻¹, diameter of 22 nm), trimethyloctylammonium bromide (C₈TAB), dodecyltrimethylammonium bromide (C₁₂TAB), hexadecyltrimethylammonium bromide (C₁₆TAB), sodium dodecyl sulfate (SDS), tetra(ethylene glycol)monododecyl ether (C₁₂E₄), and sodium chloride were purchased from Sigma-Aldrich (St. Louis, MO). The nematic thermotropic LC 4-cyano-4'-pentylbiphenyl (5CB) was purchased from TCI America (Portland, OR). Rhamnolipids, 90% pure (mixture of glycolipids purified from *Pseudomonas aeruginosa*) were purchased from AGAE Technologies (Corvallis, OR). All chemicals were used without any purification unless otherwise noted. Glass

slides for microscopy measurements were obtained from ThermoFisher Scientific (Rockford, IL). Deionized water with an electrical resistivity of 18.2 m Ω .cm was used in all experiments.

Preparation of nanoparticle-surfactant complexes. Nanoparticle-surfactant complexes were prepared by following a procedure adapted from that reported by Kirby, et. al.⁵⁷ Briefly, the commercial silica dispersion Ludox TMA was diluted with deionized water to obtain a dispersion of 20 wt.% silica nanoparticles. In this case, silica nanoparticles were dispersed using an ultrasound probe operating at an amplitude of 50% for 5 min. Stock solutions of 0.02 mM C_nTAB were prepared in 20 mM NaCl. An equal volume of surfactant solution (10 mL) was added drop-by-drop to the silica nanoparticle dispersion and mixed using an ultrasonic bath to prevent particle aggregation and favor surfactant adsorption and distribution over the nanoparticle surface. The final dispersion consisting of 10 wt.% silica nanoparticles and 0.01 mM C_nTAB in 10 mM NaCl solution was allowed to mix in the ultrasonic bath for 30 min. Prior to LC emulsion preparation, SiO₂/C_nTAB dispersions were aged for 4 days to allow the system to equilibrate and ensure a uniform distribution of surfactant over the nanoparticle surface. Based on the relative concentrations of silica nanoparticles and C_nTAB surfactants in the suspension, we estimate the C_nTAB coverage of the nanoparticle surface to be approximately 0.01%, which is significantly lower than saturation surface coverage (see Supporting Information for additional discussion).

Dynamic interfacial tension measurements. Dynamic interfacial tension measurements were obtained using an optical contact angle tensiometer OCA 15 EC (DataPhysics instruments, Filderstadt, Germany). This instrument utilizes the pendant drop method to calculate the

interfacial tension. A drop of 5CB (10 µL) was formed at the needle tip inside a cuvette filled with either 10 mM NaCl aqueous solution, 0.01 mM C_nTAB solution (10 mM NaCl), 10 wt.% SiO₂ nanoparticle dispersion (10 mM NaCl), or SiO₂/C_nTAB complexes (10 wt.% SiO₂, 0.01 mM C_nTAB, 10 mM NaCl). Images of the drop were acquired by an integrated digital camera at a frame rate of 20 frames per second (fps) and a resolution of 752 x 480 pixels. Subsequently, the software (SCA 20) recorded the geometry of the drop and the Young-Laplace equation was used to determine the interfacial tension. Interfacial tension data was collected at a speed of 4 measurements per minute and the equilibrium time was 1 hour for each drop. All experiments were carried out at 24 °C and the reported values represent the means and standard deviations of three different measurements.

Preparation of LC emulsions. LC-in-water emulsions were prepared by emulsifying 4 μL of nematic 5CB in 1.996 mL of an aqueous 10 mM NaCl dispersion containing 10 wt% of SiO₂/C_nTAB complexes or bare SiO₂ nanoparticles using homogenizer (Fisherbrand Laboratory Homogenizer, Model 125) for 1 min at 10,000 rpm. In addition, LC emulsions without emulsifiers were prepared for control experiments by homogenizing 4 µL 5CB in 1.996 mL of a 10 mM NaCl aqueous solution. Emulsions consisting of bare LC droplets were used within one hour of preparation. Here we note that, in our initial experiments, we executed a design of experiments where we varied the nanoparticle concentration, LC-to-water ratio, and homogenization time to determine the most useful procedure for LC emulsion preparation, selecting the procedure outlined above. Under these conditions, we estimate saturation coverage of the LC droplets with SiO₂/C_nTAB complexes (see Supporting Information for additional discussion).

Evaluation of emulsion stability by droplet size measurements. The colloidal stability of LC emulsions was assessed by measuring LC droplet size distributions with an Olympus BX51 optical microscope equipped with a 100x objective. Bright field micrographs of the LC droplets were captured by a Canon EOS Rebel T1i camera connected to a computer and controlled through Digital Photo Professional imaging software version 4.13.10. Droplet size distributions were determined for LC emulsions stabilized by SiO₂/C_nTAB complexes and LC emulsions prepared with bare SiO₂ nanoparticles (i.e., not mixed with C_nTAB surfactants) as a control sample. These measurements were obtained at different time points over a period of 90 days for SiO₂/C_nTAB-stabilized LC emulsions or 30 days for the control samples. Before optical characterization, the LC emulsions were hand-mixed by shaking gently to disperse the LC droplets. In both scenarios, 4 µL of LC emulsion was added to 20 µL of deionized water previously deposited onto a glass slide. After 5 minutes, bright field micrographs were acquired. The surface average diameter $D_{[3,2]}$ was calculated by analysis of at least 100 droplets for each sample using Image J software. Frequency histograms that present LC droplet size distributions were constructed using Statgraphics Centurion 18 software. The reported values represent average diameters and standard deviations of at least three different experiments on triplicate samples. The $D_{[3,2]}$ was determined by the following equation:^{38,59}

$$D_{[3,2]} = \frac{\sum_{i} N_{i} D_{i}^{3}}{\sum_{i} N_{i} D_{i}^{2}}$$

where, N_i is the total number of droplets with diameter D_i . The droplet size distribution of bare LC droplets was also measured. In this case, the bare LC emulsion sample was not diluted with deionized water. Thus, 20 μ L of bare LC emulsion was deposited directly onto a glass slide.

Because bare LC emulsions are only stable over short time periods, all measurements were made within one hour of preparation.

Optical characterization of LC droplets. Ordering transitions in LC droplets were characterized using an Olympus BX51 optical microscope equipped with a 100x objective under a cross polarizer. The LC droplets were exposed to a set of amphiphilic analytes, including anionic SDS, cationic C₁₂TAB, nonionic C₁₂E₄, and rhamnolipid. These experiments were performed by exposure of individual samples of emulsions to a fixed and predetermined set of surfactant concentrations; surfactant concentration was not added or varied continuously in these experiments. The LC droplet configuration at each surfactant concentration was monitored to determine the lowest of the tested concentrations that lead to a change from the initial bipolar configuration to a "non-bipolar" configuration in > 70% of at least 100 LC droplets (see text below). A 4 µL aliquot of each treated emulsion sample was analyzed at each experimental condition (i.e., surfactant concentration and emulsion storage time); these experiments were conducted in duplicate. All surfactant solutions were prepared in deionized water. Stock solutions of SDS, C₁₂TAB, C₁₂E₄, and rhamnolipid were prepared at 1 mM, 3 mM, 1 mM, and 100 µg/mL, respectively. Optical characterization was performed for LC emulsions stabilized by SiO₂/C_nTAB complexes and two control samples: LC droplets dispersed in 10 mM NaCl aqueous solution and LC emulsions prepared with bare SiO₂ nanoparticles (i.e., not mixed with C_nTAB surfactants). Polarized light micrographs were acquired at different time points over a period of 90 days for stabilized LC droplets exposed to the surfactant SDS. Because we found that the ordering transitions induced by SDS in the SiO₂/C_nTAB-stabilized LC droplets were generally consistent at each surfactant concentration tested over this period, we performed

subsequent experiments with the surfactants C₁₂TAB and C₁₂E₄ only on day 1 after emulsion preparation. In the case of the experiments with the biosurfactant rhamnolipid, the optical characterization was conducted after 16 days of emulsion storage time. The optical characterization of bare LC droplets was conducted within one hour of preparation. Before optical characterization, the stabilized LC emulsions were hand-mixed by shaking gently to disperse the LC droplets (this procedure was performed from day 1). For experiments with SDS, C₁₂TAB, and C₁₂E₄, 4 μL of LC emulsion were added to 20 μL of surfactant solution previously deposited onto a glass slide. Prior to the experiments, the glass slides were rinsed using ethanol and water and then dried under nitrogen, for at least three cycles. After 10 minutes, polarized light micrographs were acquired. For experiments involving rhamnolipid, 40 μL of stabilized LC emulsion were mixed with 200 μL of the rhamnolipid solution. This mixture was aged for at least 1 hour before optical characterization of LC droplets. Here, 20 μL of the mixture were deposited onto a glass slide, and polarized light micrographs were obtained after 5 minutes.

Results and Discussion

We selected SiO₂ nanoparticles and C_nTAB surfactants as model components for our studies for several reasons. First, SiO₂/C_nTAB complexes have been used in previous studies to stabilize a broad range of conventional, isotropic oil-in-water emulsions. ^{49,50,52,54,60-63} SiO₂ nanoparticles alone do not generally accumulate at oil-water-interfaces because they are hydrophilic. ^{56,63} However, because they are negatively charged, combining them with cationic surfactants can increase hydrophobicity and thus promote adsorption. ^{49,50,52,64} Second, as opposed to emulsions formed by SiO₂ (or other) nanoparticles alone, this mixed nanoparticle-surfactant system also provides opportunities to vary composition and surfactant structure (e.g.,

tail length) in ways that have the potential to impact both colloidal stability *and* the sensitivity of the response of the LC droplets to added analytes. This hypothesis is based on observations in past studies showing (i) that the adsorption of SiO₂/C_nTAB complexes to air-water interfaces depends upon surfactant tail length, with the magnitude of surface tension decreasing monotonically with increasing surfactant tail length,⁵⁷ and (ii) that the orientation of LCs in thin films¹¹ or emulsion droplets^{3,35,36} is strongly influenced by the structures of the tails of surfactants that adsorb from aqueous solution, with longer tails generally leading to orientational transitions at lower bulk surfactant concentrations.^{11,35} Finally, we reasoned that a stabilizing system based on a formulation using cationic surfactants would provide opportunities to decorate LC droplet surfaces with particles that have the potential to permit discrimination amongst other charged amphiphiles, providing a possible means to further modulate response and introduce selectivity into these systems. We provide additional detail and discussion on each of these key points in the sections below.

Characterization of the colloidal stability of LC-in-water Pickering emulsions

We began our work by characterizing the colloidal stability of LC droplets stabilized by nanoparticle-surfactant complexes formed using monodisperse SiO₂ nanoparticles (22 nm in diameter) and three different C_nTAB surfactants of different alkyl tail lengths (n = 8, 12, or 16). We prepared LC-in-water emulsions of 5CB in the presence of SiO₂/C_nTAB complexes suspended in 10 mM NaCl (0.2% 5CB, v/v), and then characterized the colloidal stability of the emulsions as a function of storage time over a period of 90 days. We used media containing NaCl in these experiments following the procedure outlined by Kirby et. al.⁵⁷

We used two complementary approaches to characterize colloidal stability: (i) monitoring changes in the turbidity of the emulsions and (ii) characterizing changes in LC droplet size over time. Figure 3A shows representative photographs of SiO₂/C_nTAB-stabilized LC emulsions after 30 days of storage time. The emulsions remained turbid over this period and phase separation was not observed. Although sedimentation of the LC droplets was observed with time as a result of differences in density between the LC and the water phases (Figure 3A, bottom), the droplets did not coalescence over this time and were readily re-dispersed after gentle manual shaking (Figure 3A, right panel). As shown in the photographs, the three C_nTAB surfactants used to form the nanoparticle-surfactant complexes led to similar levels of colloidal stability in this qualitative context. In contrast, as shown in Figure 3A, bare LC droplets (formed by creating conventional LC-in-water emulsions in the absence of nanoparticle-surfactant complexes or other stabilizers) coalesced within hours of emulsion preparation (see also Supporting Information, Figure S1). In these cases, the LC and water phases completely separated within 48 hours of emulsion preparation (Figure 3A, right panel).

We also measured droplet size distributions for SiO₂/C_nTAB-stabilized LC emulsions over a period of 90 days. As shown in Figure 3B, droplet sizes did not change significantly under these conditions and we did not observe any apparent differences in behavior as a function of C_nTAB length (diameters ranged from 3.0 μm to 3.9 μm for SiO₂/C₈TAB, 2.8 μm to 3.6 μm for SiO₂/C₁₂TAB, and 3.0 μm to 3.5 μm for SiO₂/C₁₆TAB complexes; see Supporting Information, Figure S2, Table S1). When combined, the results of these experiments demonstrate the robust colloidal stability of this LC Pickering emulsion system. Here we note that, as a control, we also prepared LC emulsions using SiO₂ nanoparticles without added C_nTAB cationic surfactant. We found the nanoparticles to stabilize the emulsions for at least 30 days (Figure 3B). As discussed

in greater detail below, however, other experiments using polarized light microscopy to characterize optical transitions in these materials demonstrated that the presence of C_nTAB had additional positive impacts on droplet sensitivity. As a result, we focus our attention in the sections below on the stabilization of LC emulsions using SiO₂/C_nTAB complexes. Finally, we

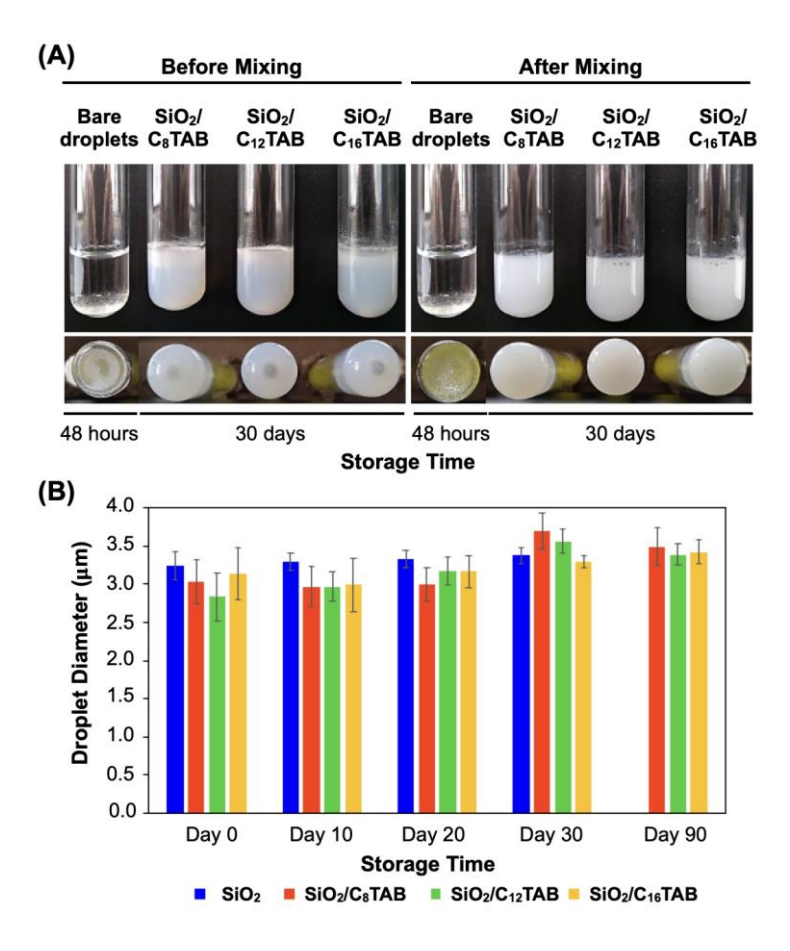


Figure 3. (A) Images of LC-in-water emulsions prepared using SiO₂/C_nTAB complexes obtained after a storage time of 30 days upon emulsion preparation, before (left) and after (right) hand-mixing. As a reference, LC emulsions consisting of bare LC droplets were visibly phase-separated by 48 hours after preparation and could not be re-dispersed by hand-mixing. (B) Droplet diameter as a function of storage time of Pickering LC emulsions prepared using SiO₂ nanoparticles complexed with C₈TAB (red bars), C₁₂TAB (green bars) or C₁₆TAB (yellow bars) surfactants. After the day of emulsion preparation (labeled Day 0), the emulsions were hand-mixed prior to droplet size measurements to disperse sedimented LC droplets. Control measurements of LC droplet diameters of Pickering LC emulsions prepared using SiO₂ nanoparticles with no cationic C_nTAB surfactant (blue bars) up to 30 days after preparation are also shown. The reported values represent the average and standard deviations of three independent experiments with triplicate samples.

note that, to complement the emulsion stability studies described here, we performed interfacial tension (IFT) measurements to characterize the adsorption of the SiO₂/C_nTAB complexes to the LC-water interface. The results of our IFT measurements (see Supporting Information, Figure S3) show that the overall change in the magnitude of the IFT promoted by these complexes was only slightly influenced by surfactant tail length, with the largest effect observed for the SiO₂/C₁₆TAB surfactant complexes. These results are consistent with our observations that the three nanoparticle-surfactant complexes investigated here adsorb to the LC-water interface and are effective LC emulsion stabilizers.

Ordering transitions induced by SDS in LC droplets stabilized by SiO₂/C_nTAB complexes

We performed additional experiments to characterize optical transitions in SiO₂/C_nTAB-stabilized LC droplets before and after exposure to aqueous solutions of target amphiphiles. For these experiments, we prepared Pickering LC emulsions as described above and used polarized light microscopy to characterize ordering transitions in the LC droplets and determine the lowest amphiphile concentration required to induce a change from the initial bipolar state to a "non-bipolar" state (see text below for additional details). For all studies described below, we maintained the concentration of the C_nTAB surfactants used to stabilize the droplets constant at 0.01 mM because this low C_nTAB concentration does not, itself, promote ordering transitions in LC droplets. We found LC droplets stabilized by SiO₂/C_nTAB complexes (10 wt% / 0.01 mM, in 10 mM NaCl) to exhibit 'bipolar' configurations similar to those observed in past studies of bare droplets dispersed in water.³⁵ In the bipolar configuration, the director of the LC is aligned tangentially to the droplet interface and two opposite point defects form, as shown in the cartoon in Figure 4A. These bipolar droplets have the optical appearance shown in Figure 4B when viewed by polarized light microscopy.

These bipolar SiO₂/C_nTAB-stabilized droplets underwent rapid and diagnostic 'bipolar-to-radial' transformations upon addition of 1.0 mM of SDS. In the 'radial' configuration, the director of the LC is aligned perpendicular to the droplet surface and a single defect forms at the center of the droplet (see Figure 4A).^{7,35} These radial droplets have the distinct optical appearance shown in Figure 4C when observed under a polarized light microscope. The bipolar-to-radial ordering transitions observed here and shown in Figure 4 are consistent with observations from past studies of LC emulsion droplets upon exposure to SDS.^{6,35} These results demonstrate that the adsorption of SiO₂/C_nTAB complexes at the aqueous/LC droplet interface does not interfere with other commonly observed amphiphile-induced ordering transitions of the LC.

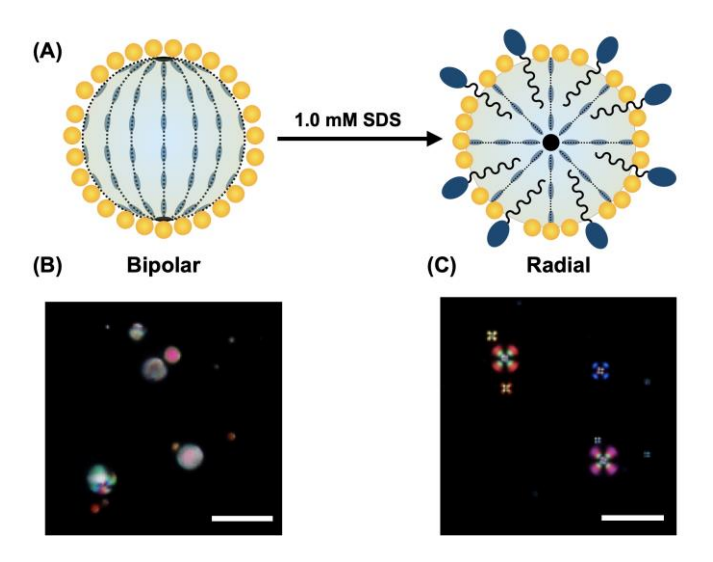


Figure 4. Ordering transitions of LC droplets stabilized by nanoparticle-surfactant (SiO₂/C_nTAB) complexes. (A) Schematic illustration of SiO₂/C_nTAB-stabilized LC droplets with the LC director profiles (dotted lines) in the bipolar (left) and radial (right) configurations, before and after addition of surfactant, respectively. The characteristic defects for each configuration are represented as black dots. (B) Polarized-light micrographs of SiO₂/C₁₆TAB-stabilized LC droplets dispersed in water in the bipolar configuration before addition of the surfactant SDS and (C) in the radial configuration after addition of 1.0 mM SDS. Scale bars correspond to 20 μm.

We next performed experiments to characterize the influence of SDS concentration on ordering transitions in SiO₂/C_nTAB-stabilized LC droplets. As part of these studies, we sought to determine the lowest bulk SDS concentration at which the addition this analyte could trigger useful changes in anchoring in larger populations of droplets and, thus, produce a diagnostic optical response in this experimental system. We note again that past studies on LC thin films¹¹ and bare LC droplets^{3,36} have shown that the orientation of 5CB in the presence of aqueous solutions containing amphiphiles is strongly influenced by the length and/or structure of tail groups. For C_nTAB surfactants, increasing the tail length from n = 8 to n = 16 was reported to lead to planar-to-homeotropic (or tangential-to-perpendicular) changes in the orientation of 5CB thin films at lower bulk surfactant concentrations, a result that was attributed to increased penetration of the longer surfactant tails of C₁₆TAB into the 5CB-water interface. ¹¹ We first aimed to determine whether varying the length of the tail of the C_nTAB surfactant used to help stabilize the LC droplets could influence the sensitivity of the LC response to SDS. For these experiments, we characterized ordering transitions in SiO₂/C_nTAB-stabilized LC emulsions upon exposure to SDS using LC emulsions that were either freshly prepared or aged for up to 90 days before use.

Figure 5 shows representative optical micrographs obtained for LC droplets one day after preparation upon exposure to increasing concentrations of SDS up to 1 mM (additional results of experiments performed using 90-day droplets were similar to the results obtained using these 1-day droplets, and are shown in Figure S4). Inspection of panels A-C of Figure 5 reveals exposure to SDS to lead to changes in the optical appearances of SiO₂/C_nTAB-laden LC droplets in all samples (n = 8, 12, and 16). These results also reveal significant differences in the concentrations of SDS at which these transformations are observed to occur. Overall, our results show that

increasing the tail length of the C_nTAB used to form the stabilizing complex from n=8 to n=16 leads to a more sensitive response of the LC. We found that for LC droplets stabilized using complexes formed using $C_{16}TAB$, a concentration of SDS of 0.2 mM was sufficient to induce a bipolar-to-radial ordering transition in ~100% of the droplets (Figure 5C). This threshold

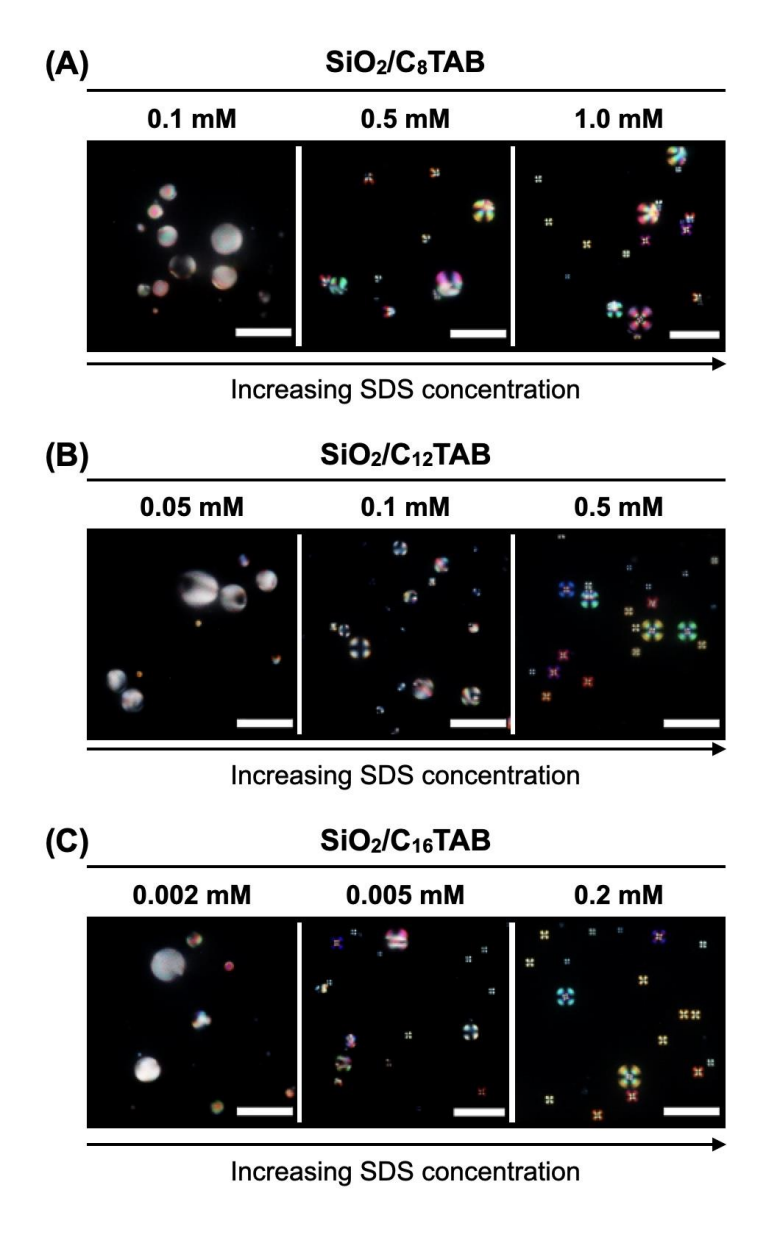


Figure 5. Optical micrographs showing LC ordering transitions triggered by the addition of increasing concentrations of the anionic surfactant SDS to LC emulsions stabilized using (A) SiO₂/C₈TAB, (B) SiO₂/C₁₂TAB, or (C) SiO₂/C₁₆TAB. These representative results were obtained using emulsions 1 day after preparation (see text). Scale bars correspond to 20 μm.

concentration increased to 0.5 mM for shorter-tailed C₁₂TAB-stabilized complexes (Figure 5B), and for C₈TAB-stabilized complexes, complete and uniform bipolar-to-radial transitions were not observed even at 1 mM SDS (under these conditions, we often observed mixtures of radial droplets and other droplet configurations, as well as some bipolar droplets; see Figure 5A and additional discussion below).

Here we note that the results shown in Figure 5 are representative results, selected for clarity of discussion from experiments performed over a wider range of (i) SDS concentrations and (ii) droplet aging periods (from 1 to 90 days after emulsion preparation). The results of those additional experiments are summarized in Table 1, and reveal differences in both the SDS concentrations at which ordering transitions in LC were observed to occur and the range of different optical textures observed in these droplets under each condition (see also Supporting Information, Table S2). In addition to the radial configuration described above, spherical LC droplets suspended in water can exhibit other optical configurations, including so-called 'escaped radial' and 'pre-radial' configurations. 3,35,41 Past studies demonstrate that when LC droplets are exposed to amphiphiles, the type of configuration that is subsequently observed is often dependent upon the concentration of the amphiphile.^{3,35} In general, escaped radial and pre-radial configurations are observed at lower amphiphile concentrations, and radial configurations are most often observed at or near concentrations that lead to amounts of adsorbed amphiphile approaching droplet surface saturation. In our studies, we observed that further lowering the concentration of SDS, at each SiO₂/C_nTAB condition, often led to populations of droplets that contained mixtures of one or more of these droplet configurations. In Table 1, we use designations of B, R, and M to represent observations of completely bipolar (B), completely radial (R), or mixtures (M) of configurations, respectively. For clarity, we note that M is used

here to indicate populations of droplets that were neither 100% bipolar nor 100% radial, but that instead contained droplets in at least two or more of the bipolar, pre-radial, escaped radial, and radial configurations. We also adopted an operational criterion for categorizing the apparent sensitivity of LC response based on the lowest concentration of amphiphile for which more than 70% of the droplets observed in a sample exhibited ordering transitions that were 'not bipolar' (that is, a condition containing a mixture of configurations in which >70% of droplets were no longer observed to be in their initial bipolar state was considered here to have undergone a meaningful and diagnostic "bipolar-to-non-bipolar" transition that can be used to define a threshold useful for describing and comparing overall droplet sensitivities).

Table 1. Ordering transitions of SiO₂/C_nTAB-stabilized LC droplets triggered by addition of increasing concentrations of the anionic surfactant SDS at different concentrations and emulsion storage times. The designations B, R, and M represent bipolar, radial, or a mixture of configurations, respectively. M denotes a mixed condition for which more than 70% of the droplets observed in a sample exhibited ordering transitions that were not bipolar (see text).

SDS Concentration (mM)												
Day	SiO ₂ /C ₈ TAB				SiO ₂ /C ₁₂ TAB				SiO ₂ /C ₁₆ TAB			
	0	0.2	0.5	1	0	0.1	0.5	1	0	0.005	0.05	0.2
0	В	M	M	M	В	M	M	M	В	M	M	R
1	В	В	M	M	В	M	M	M	В	M	M	R
2	В	В	M	M	В	M	M	M	В	-	M	R
3	В	В	M	M	В	M	R	R	В	-	M	R
10	В	В	M	M	В	M	R	R	В	M	M	R
20	В	В	M	M	В	M	R	R	В	M	M	R
30	В	В	M	M	В	M	R	R	В	M	M	R
90	В	В	M	M	В	M	R	R	В	M	M	R

For droplets stabilized using complexes formed with C₈TAB, the threshold for "bipolar-to-non-bipolar" ordering transitions upon exposure to SDS was determined to be 0.5 mM (e.g., Figure 5A; center panel). For droplets stabilized using complexes formed using longer-tailed C₁₂TAB, this threshold was achieved at a lower concentration of 0.1 mM SDS (Figure 5B; center panel). Finally, for emulsions stabilized with complexes formed using C₁₆TAB, >70% of droplets were observed to undergo diagnostic "bipolar-to-non-bipolar" ordering transitions at substantially lower concentrations of SDS, as low as 5 μM. Overall, these results show that SiO₂/C_nTAB-stabilized LC droplets can detect and report the presence of SDS after up to 90 days of storage time, and that the operational sensitivity of these droplets is influenced significantly by the length of the tails of the surfactant used to help colloidally stabilize them.

We note that the threshold concentration that can be used to reliably report the presence of SDS using SiO₂/C₁₆TAB (5 μM, or 0.005 mM) is substantially lower than that of bare LC droplets under otherwise identical conditions (0.3 mM SDS; see Figure S5). We note further that samples of droplets stabilized by SiO₂/C₁₆TAB undergo diagnostic transitions at a concentration of SDS (5 μM) that is lower than that required using droplets stabilized with C₈TAB and C₁₂TAB. The reasons for this large difference in behavior are not completely clear, but this is likely a consequence of interactions between both the head and tail groups of these cationic surfactants and SDS and/or the LC interfaces in these materials. Overall, we speculate that the cationic nature of these C_nTAB surfactants promotes interactions with anionic SDS that enhance the recruitment of SDS to the LC interface, thus contributing to improved overall sensitivity. It is also possible that the formation of C_nTAB/SDS ion pairs^{65,66} could effectively increase the areal density of surfactant tails in contact with the LC, thereby leading to ordering transitions that occur at lower SDS concentrations. While these interactions would be expected to occur for

mixtures of SDS and C_nTAB regardless of tail length, the increased length of the hydrocarbon tails in C₁₆TAB would likely promote changes in the orientation of the LC at these aqueous/LC interfaces more effectively than those of C₈TAB and C₁₂TAB (as mentioned above, increasing tail length has been reported to increase the extent of penetration of C_nTAB surfactant tails into LC-water interfaces at lower bulk surfactant concentrations). 11 We note that we also performed experiments using LC droplets stabilized by SiO₂ nanoparticles without added C_nTAB surfactant. Under these conditions, 0.5 mM SDS was required to trigger changes in LC droplet configuration (see Figure S5 and Table S3)—a concentration that is higher than the concentration required to trigger these changes in bare LC droplets (0.3 mM). We conclude that, although SiO₂ nanoparticles alone can effectively stabilize LC emulsions and do not abrogate their functional behaviors in the context of sensing, they do reduce sensitivity. These results provide further support for the view that the cationic C_nTAB surfactants play important roles in governing the response of our LC droplets. Other contributions or combinations of electrostatic and hydrophobic interactions are also possible and likely in these complex and dynamic systems. However, the physical pictures proposed here are generally consistent with the results above and the results of additional experiments performed using cationic and nonionic surfactants, described in greater detail below.

Ordering transitions induced by other synthetic and bacterial surfactants

We performed additional experiments with SiO₂/C_nTAB-stabilized LC droplets using C₁₂TAB and C₁₂E4 as additional cationic and neutral analytes. SDS, C₁₂TAB, and C₁₂E4 differ in the structure and charge of their polar head groups (Figure 2), but each has hydrocarbon tails that are 12 carbons long. This set of model surfactants can thus be used to provide insight into

the influence of charge on the responses of LC droplets. Past studies using LC thin films have shown that the nature of the surfactant head group does not directly impact LC anchoring transitions significantly, but can influence the interfacial density of the adsorbed surfactant through head group repulsion.¹¹ In view of the results described above, we hypothesized that the presence of cationic surfactants in our SiO₂/C_nTAB-stabilized LC droplet could influence the sensitivity of the LC response to anionic, cationic, and nonionic surfactants and, thereby, potentially provide a basis for introducing some degree of selectivity to these systems. Representative polarized light micrographs of LC droplets exposed to varying concentrations of C₁₂TAB and C₁₂E4, similar to those shown above for exposure to SDS in Figure 5, are shown in Figure S6 and Figure S7 (see also Table S4 and Table S5). For clarity, those tabular results are also summarized and depicted graphically in Figure 6, which indicates the lowest concentrations of SDS, C₁₂TAB, and C₁₂E4 at which we observed "bipolar-to-non-bipolar" ordering transitions in >70% of the LC droplets observed in a sample at each SiO₂/C_nTAB condition tested (see Materials and Methods for additional details). Inspection of the results presented in Figure 6 reveals that, for the detection and reporting of added C₁₂TAB (panel B), the LC response is dependent upon the hydrocarbon tail length of the C_nTAB surfactant used to form the stabilizing complexes, as observed for experiments using SDS (panel A; see also Figure 5, above). The surfactant concentration required to trigger an LC ordering transition decreased monotonically with increasing tail length over the range of 2.0 mM to 1.3 mM. This range of concentrations is smaller than that observed for the response to SDS, but is equal to or higher than the concentration of C₁₂TAB otherwise required to promote transitions in bare LC droplets (1.3 mM; as indicated by the dotted line in panel B; see also Figure S8 and Table S4). We interpret this result to reflect several possibilities for the adsorption of C₁₂TAB that could lead to the

depletion of the overall effective concentration of added C₁₂TAB that is available to adsorb at the aqueous/LC interface. First, it is possible that the presence of additional cationic surfactant already situated at the interfaces of these SiO₂/C_nTAB-stabilized LC droplets would introduce

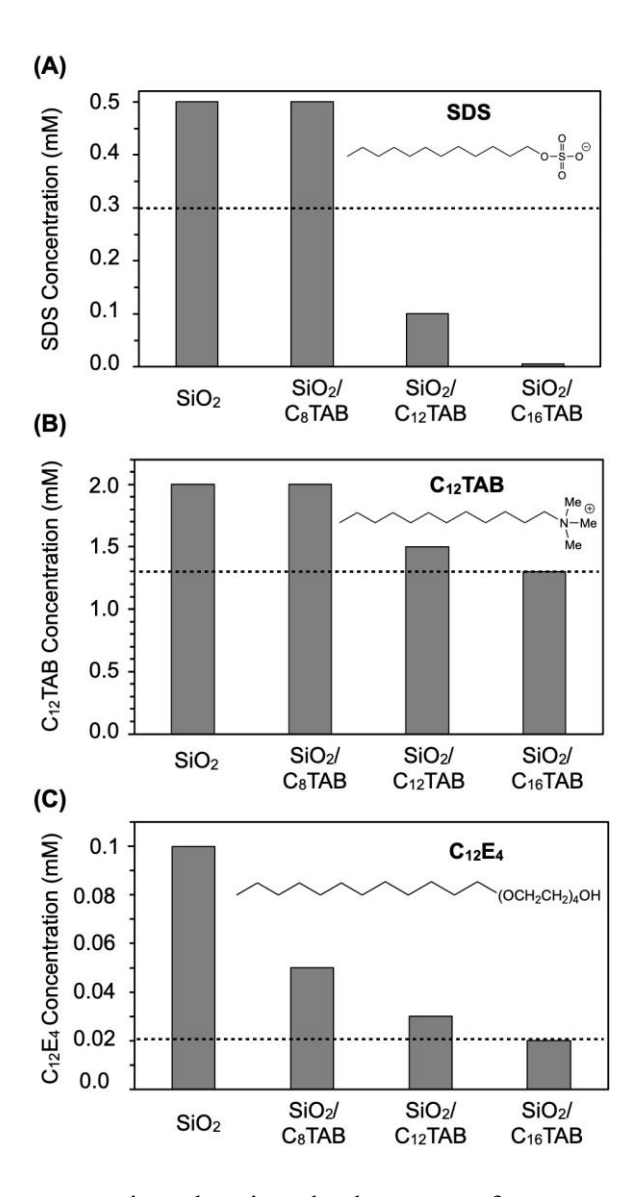


Figure 6. Graphical representation showing the lowest surfactant concentration required to trigger "bipolar-to-non-bipolar" ordering transitions in Pickering stabilized LC droplets in contact with (A) anionic SDS, (B) cationic C₁₂TAB, and (C) nonionic C₁₂E₄. Data are extracted from results shown in Table S2, Table S3, Table S4, and Table S5; see main text for details. The dotted lines represent the surfactant concentration determined to trigger an LC ordering transition in bare LC droplets dispersed in 10 mM NaCl aqueous solution. Surfactant structures are also shown.

repulsive ionic interactions that could influence or hinder the transport of additional C₁₂TAB to the aqueous/LC interface (i.e., the opposite of what was observed and discussed above, and summarized in panel A, for results in which anionic SDS was used as an analyte). Second, it is also possible that C₁₂TAB could partially adsorb to the surfaces of the nanoparticles stabilizing the droplets; this possibility is supported by the low surface coverage of the existing surfactant on these particles, as mentioned above. Finally, C₁₂TAB could also adsorb to the surfaces of non-adsorbed nanoparticles that are in excess in the suspension. Consistent with these physical pictures, the results of experiments using LC droplets stabilized by SiO₂ nanoparticles only (no C_nTAB, see also Figure S8) revealed threshold concentrations for response that were higher than those observed in the presence of SiO₂/C_nTAB complexes, possibly due to the preferential or partial adsorption of C₁₂TAB to the surfaces of the bare nanoparticles, which would deplete the overall effective concentration of added C₁₂TAB available to adsorb at the aqueous/LC interface.

Panel C of Figure 6 shows the equivalent set of results for experiments in which the nonionic surfactant C₁₂E₄ was used as a model analyte. These results reveal a similar increase in the sensitivity of the LC droplet response as the length of the tail of the C_nTAB surfactant used to form the stabilizing nanoparticle/surfactant complexes was increased, as observed for both SDS and C₁₂TAB. We note that the range of surfactant concentrations required to trigger these responses (from 0.05 mM to 0.02 mM) was also equal to or higher than that required to trigger an ordering transition in bare LC droplets (0.02 mM; as indicated by the dotted line in panel C; see also Figure S9 and Table S5), a result that is, overall, consistent with the behavior observed in experiments using C₁₂TAB as a model analyte, as discussed above. This range also occurs below the threshold concentration for a triggered response in LC droplets stabilized using bare

SiO₂ nanoparticles, again consistent with the well established ability of this nonionic surfactant to absorb onto SiO₂ surfaces.^{67,68}

Overall, the results above show that the analyte concentration required to induce an ordering transition in SiO₂/C_nTAB-stabilized LC droplets decreases monotonically with increasing C_nTAB tail length for all surfactants tested, revealing a straightforward approach that can be used to tune the sensitivities of these LC droplets. These results also show that, while SiO₂ nanoparticles alone can confer colloidal stability to LC droplets without preventing their ability to respond to aqueous amphiphiles, the response of the LC is generally enhanced when SiO₂/C_nTAB complexes are used. Notably, our results also show that LC emulsions stabilized using SiO₂/C₁₆TAB complexes respond to SDS at concentrations that are much lower (in the micromolar range) as compared to the concentrations required when cationic or nonionic analytes are used (in the millimolar range). These results are, in general, consistent with the view that the SiO₂/C₁₆TAB complexes hosted at these LC droplet interfaces could help preferentially recruit anionic amphiphiles. This result hints at strategies that may be useful for the design of LC droplets that can exhibit additional degrees of selectivity based on amphiphile structure or charge. Additional experiments and studies of LC droplet response in solutions containing mixtures of multiple different analytes were not pursued as part of this current study, and would be needed to evaluate this additional hypothesis more completely.

Based on the results above using model synthetic surfactants, we performed a final series of experiments to explore the potential of these LC Pickering emulsions to detect the biosurfactant rhamnolipid in aqueous solutions. Rhamnolipid is an amphiphilic virulence factor produced by the bacterial pathogen *P. aeruginosa* under the control of quorum sensing.⁵⁸ We previously reported that bare LC droplets can detect rhamnolipid in defined aqueous media and

when deployed in the presence of live bacteria, and thus report the onset of virulence in bacterial cultures, at biologically relevant concentrations of \sim 6 µg mL⁻¹. 36 Figure 7 shows a plot of the lowest concentrations of rhamnolipid required to induce ordering transitions in LC droplets for Pickering emulsions formed using SiO₂/C₈TAB, SiO₂/C₁₂TAB, and SiO₂/C₁₆TAB formulations (see Figure S10 for corresponding polarized light micrographs arising from these experiments, and Table S6). Our results demonstrate that LC droplets stabilized by SiO₂/C₁₆TAB can respond to and report the presence of rhamnolipid at concentrations of 5 µg mL⁻¹. These formulations thus provide a platform for the sensing and reporting of bacterial virulence products in aqueous solutions with sensitivities that are similar to those reported for bare droplets, but with levels of colloidal stability that far exceed those of unprotected, bare droplet systems.

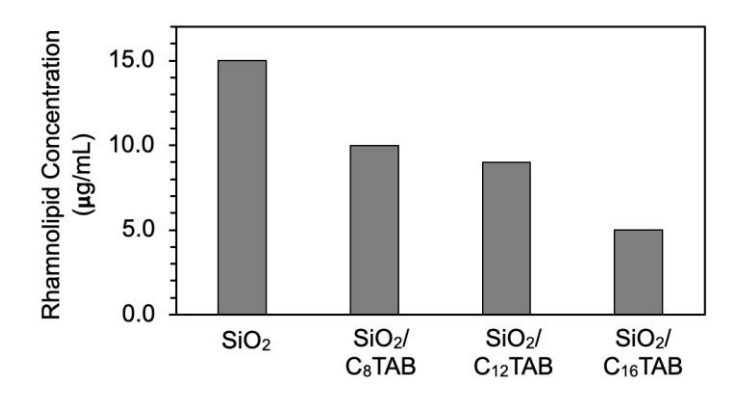


Figure 7. Graphical representation showing the lowest rhamnolipid concentration required to trigger a "bipolar-to-non-bipolar" ordering transition in Pickering LC emulsions stabilized using SiO₂/C_nTAB complexes. Data are extracted from results shown in Table S6; see main text for details.

Conclusions

LC emulsions can detect and report the presence of amphiphilic analytes in aqueous environments with remarkable sensitivity, but the practical utility of these droplet-based sensors

is limited by the fact that they are not colloidally stable. Here, we have reported a Pickering stabilization strategy based on the use of nanoparticle-surfactant complexes, which can provide remarkable colloidal stability to LC droplets for at least three months. These nanoparticle-surfactant complexes are comprised of SiO₂ nanoparticles and one of three different C_nTAB surfactants of different alkyl tail lengths (n = 8, 12, or 16). Our results reveal that these nanoparticle-surfactant complexes adsorb to LC-water interface and lead to similar levels of colloidal stability, demonstrating that they are effective LC emulsion stabilizers.

We also demonstrated that these SiO₂/C_nTAB-stabilized LC droplets undergo diagnostic bipolar-to-radial ordering transitions upon exposure to anionic, cationic, and nonionic amphiphilic analytes. The analyte concentrations required to induce ordering transitions in these stabilized LC droplets decreased monotonically with increases in the hydrocarbon tail length of the C_nTAB surfactant used to form the SiO₂/C_nTAB stabilizing complex. In general, increasing the C_nTAB tail length from n = 8 to n = 16 led to a more sensitive response of the LC to the model analytes SDS, C₁₂TAB, and C₁₂E₄, demonstrating that this approach could be used to tune the sensitivities of the stabilized LC droplets more broadly, and suggesting that this approach could be general. Our results also reveal significant differences in the concentrations of the anionic surfactant SDS required to trigger LC ordering transitions (in the micromolar range) when compared to the cationic $C_{12}TAB$, and the nonionic $C_{12}E_4$ (in the millimolar range), hinting at the possibility of using this strategy to impart some degree of selectivity to the stabilized LC droplets. Moreover, the threshold concentration of SDS reported by the SiO₂/C₁₆TAB complex (5 μM) is two orders of magnitude lower than that required to trigger diagnostic orientational transitions in bare LC droplets, demonstrating the potential to substantially enhance the sensitivity of LC droplets using this approach. Finally, we demonstrated that these stabilized LC

droplets can be used to report the presence of rhamnolipid, a technologically useful biosurfactant produced as a virulence factor by the bacterial pathogen *P. aeruginosa*, at biologically relevant concentrations.

When combined, the results reported here support the conclusion that Pickering LC emulsions stabilized by SiO₂/C_nTAB complexes provide a useful approach for the design of responsive LC droplet-based sensors with substantially improved colloidal and shelf-life stability, as well as new opportunities for tuning and enhancing sensitivity of response. We anticipate that the exceptional colloidal stability and extended shelf-life of these Pickering emulsion formulations will open the door to the deployment of LC droplet sensors as useful and practical tools in a range of different fundamental and applied settings.

Acknowledgments. Financial support for this work was provided by the NSF through a grant provided to the Wisconsin-Puerto Rico Partnership for Research and Education in Materials [Wi(PR)2EM] at the University of Puerto Rico—Mayaguez and the University of Wisconsin—Madison (PREM; DMR-1827894) and the UW-Madison Materials Research Science and Engineering Center (MRSEC; DMR-1720415). The authors acknowledge the use of instrumentation supported by the NSF through the UW MRSEC (DMR-1720415). The authors gratefully acknowledge Dr. Benjamin Ortiz and Fengrui Wang (UW-Madison) and Dr. Aldo Acevedo, Kevin Zabala, and Lucas Capre (UPR-Mayagüez) for many helpful discussions.

Supporting Information. Plots and images providing additional qualitative and quantitative characterization of LC droplet stability and responses to aqueous amphiphiles (PDF). This material is available free of charge via the Internet.

ORCID

Claribel Acevedo-Vélez: 0000-0001-6297-7747

David M. Lynn: 0000-0002-3140-8637

References

- 1. Gupta, V. K.; Skaife, J. J.; Dubrovsky, T. B.; Abbott, N. L. Optical Amplification of Ligand-Receptor Binding Using Liquid Crystals. *Science* **1998**, *279*, 2077-80.
- 2. Brake, J. M.; Daschner, M. K.; Luk, Y.-Y.; Abbott, N. L. Biomolecular Interactions at Phospholipid-Decorated Surfaces of Liquid Crystals. *Science* **2003**, *302*, 2094-2097.
- 3. Lin, I.-H.; Miller, D. S.; Bertics, P. J.; Murphy, C. J.; De Pablo, J. J.; Abbott, N. L. Endotoxin-Induced Structural Transformations in Liquid Crystalline Droplets. *Science* **2011**, *332*, 1297-1300.
- 4. Bai, Y.; Abbott, N. L. Recent Advances in Colloidal and Interfacial Phenomena Involving Liquid Crystals. *Langmuir* **2011**, *27*, 5719–5738.
- 5. Miller, D. S.; Carlton, R. J.; Mushenheim, P. C.; Abbott, N. L. Introduction to Optical Methods for Characterizing Liquid Crystals at Interfaces. *Langmuir* **2013**, *29*, 3154-3169.
- 6. Miller, D. S.; Wang, X.; Buchen, J.; Lavrentovich, O. D.; Abbott, N. L. Analysis of the Internal Configurations of Droplets of Liquid Crystal Using Flow Cytometry. *Anal. Chem.* **2013**, *85*, 10296-10303.
- 7. Bukusoglu, E.; Bedolla Pantoja, M.; Mushenheim, P. C.; Wang, X.; Abbott, N. L. Design of Responsive and Active (Soft) Materials Using Liquid Crystals. *Annu. Rev. Chem. Biomol. Eng.* **2016**, *7*, 163-96.
- 8. Popov, P.; Mann, E. K.; Jákli, A. Thermotropic Liquid Crystal Films for Biosensors and Beyond. *J. Mater. Chem. B* **2017**, *5*, 5061-5078.
- 9. Kim, Y.-K. K.; Noh, J.; Nayani, K.; Abbott, N. L. Soft Matter from Liquid Crystals. *Soft Matter* **2019**, *15*, 6913-6929.
- 10. Wang, Z.; Xu, T.; Noel, A.; Chen, Y.-C.; Liu, T. Applications of Liquid Crystals in Biosensing. *Soft Matter* **2021**, *17*, 4675-4702.
- 11. Brake, J. M.; Mezera, A. D.; Abbott, N. L. Effect of Surfactant Structure on the Orientation of Liquid Crystals at Aqueous–Liquid Crystal Interfaces. *Langmuir* **2003**, *19*, 6436-6442.

- 12. Lockwood, N. A.; Abbott, N. L. Self-Assembly of Surfactants and Phospholipids at Interfaces between Aqueous Phases and Thermotropic Liquid Crystals. *Curr. Opin. Colloid Interface Sci* **2005**, *10*, 111-120.
- 13. Price, A. D.; Schwartz, D. K. DNA Hybridization-Induced Reorientation of Liquid Crystal Anchoring at the Nematic Liquid Crystal/Aqueous Interface. *J. Am. Chem. Soc.* **2008**, *130*, 8188-8194.
- 14. Price, A. D.; Ignés-Mullol, J.; Àngels Vallvé, M.; Furtak, T. E.; Lo, Y.-A.; Malone, S. M.; Schwartz, D. K. Liquid Crystal Anchoring Transformations Induced by Phase Transitions of a Photoisomerizable Surfactant at the Nematic/Aqueous Interface. *Soft Matter* **2009**, *5*, 2252-2260.
- 15. Hartono, D.; Xue, C.-Y.; Yang, K.-L.; Yung, L.-Y. L. Decorating Liquid Crystal Surfaces with Proteins for Real-Time Detection of Specific Protein–Protein Binding. *Adv. Funct. Mater.* **2009**, *19*, 3574-3579.
- 16. Sivakumar, S.; Wark, K. L.; Gupta, J. K.; Abbott, N. L.; Caruso, F. Liquid Crystal Emulsions as the Basis of Biological Sensors for the Optical Detection of Bacteria and Viruses. *Adv. Funct. Mater.* **2009**, *19*, 2260-2265.
- 17. Uline, M. J.; Meng, S.; Szleifer, I. Surfactant Driven Surface Anchoring Transitions in Liquid Crystal Thin Films. *Soft Matter* **2010**, *6*, 5482-5490.
- 18. Alino, V. J.; Pang, J.; Yang, K.-L. Liquid Crystal Droplets as a Hosting and Sensing Platform for Developing Immunoassays. *Langmuir* **2011**, *27*, 11784-11789.
- 19. Alino, V. J.; Sim, P. H.; Choy, W. T.; Fraser, A.; Yang, K.-L. Detecting Proteins in Microfluidic Channels Decorated with Liquid Crystal Sensing Dots. *Langmuir* **2012**, *28*, 17571-17577.
- 20. McUmber, A. C.; Noonan, P. S.; Schwartz, D. K. Surfactant–DNA Interactions at the Liquid Crystal–Aqueous Interface. *Soft Matter* **2012**, *8*, 4335-4342.
- 21. Ding, X.; Yang, K.-L. Antibody-Free Detection of Human Chorionic Gonadotropin by Use of Liquid Crystals. *Anal. Chem.* **2013**, *85*, 10710-10716.
- 22. Miller, D. S.; Abbott, N. L. Influence of Droplet Size, pH and Ionic Strength on Endotoxin-Triggered Ordering Transitions in Liquid Crystalline Droplets. *Soft Matter* **2013**, *9*, 374-382.
- 23. Yoon, S. H.; Gupta, K. C.; Borah, J. S.; Park, S.-Y.; Kim, Y.-K.; Lee, J.-H.; Kang, I.-K. Folate Ligand Anchored Liquid Crystal Microdroplets Emulsion for in vitro Detection of Kb Cancer Cells. *Langmuir* **2014**, *30*, 10668-10677.
- 24. Carter, M. C.; Miller, D. S.; Jennings, J.; Wang, X.; Mahanthappa, M. K.; Abbott, N. L.; Lynn, D. M. Synthetic Mimics of Bacterial Lipid a Trigger Optical Transitions in Liquid

- Crystal Microdroplets at Ultralow Picogram-Per-Milliliter Concentrations. *Langmuir* **2015**, *31*, 12850-12855.
- 25. Deng, J.; Liang, W.; Fang, J. Liquid Crystal Droplet-Embedded Biopolymer Hydrogel Sheets for Biosensor Applications. *ACS Appl. Mater. Interfaces* **2016**, *8*, 3928-3932.
- 26. Bao, P.; Paterson, D. A.; Harrison, P. L.; Miller, K.; Peyman, S.; Jones, J. C.; Sandoe, J.; Evans, S. D.; Bushby, R. J.; Gleeson, H. F. Lipid Coated Liquid Crystal Droplets for the On-Chip Detection of Antimicrobial Peptides. *Lab Chip* **2019**, *19*, 1082-1089.
- 27. Qi, L.; Hu, Q.; Kang, Q.; Bi, Y.; Jiang, Y.; Yu, L. Detection of Biomarkers in Blood Using Liquid Crystals Assisted with Aptamer-Target Recognition Triggered in situ Rolling Circle Amplification on Magnetic Beads. *Anal. Chem.* **2019**, *91*, 11653-11660.
- 28. Yang, X.; Zhao, X.; Liu, F.; Li, H.; Zhang, C. X.; Yang, Z. Simple, Rapid and Sensitive Detection of Parkinson's Disease Related Alpha-Synuclein Using a DNA Aptamer Assisted Liquid Crystal Biosensor. *Soft Matter* **2021**, *17*, 4842-4847.
- 29. Lavrentovich, O. D. Topological Defects in Dispersed Liquid Crystals, or Words and Worlds around Liquid Crystal Drops. *Liq. Cryst.* **1998**, *24*, 117-126.
- 30. Heppenstall-Butler, M.; Williamson, A. M.; Terentjev, E. M. Selection of Droplet Size and the Stability of Nematic Emulsions. *Liquid Crystals* **2005**, *32*, 77-84.
- 31. Sivakumar, S.; Gupta, J. K.; Abbott, N. L.; Caruso, F. Monodisperse Emulsions through Templating Polyelectrolyte Multilayer Capsules. *Chem. Mater.* **2008**, *20*, 2063-2065.
- 32. Gupta, J. K.; Zimmerman, J. S.; de Pablo, J. J.; Caruso, F.; Abbott, N. L. Characterization of Adsorbate-Induced Ordering Transitions of Liquid Crystals within Monodisperse Droplets. *Langmuir* **2009**, *25*, 9016-9024.
- 33. Bera, T.; Fang, J. Optical Detection of Lithocholic Acid with Liquid Crystal Emulsions. *Langmuir* **2013**, *29*, 387-392.
- 34. Kim, J.; Khan, M.; Park, S.-Y. Glucose Sensor Using Liquid-Crystal Droplets Made by Microfluidics. *ACS Appl. Mater. Interfaces* **2013**, *5*, 13135-13139.
- 35. Miller, D. S.; Wang, X.; Abbott, N. L. Design of Functional Materials Based on Liquid Crystalline Droplets. *Chem. Mater.* **2014**, *26*, 496-506.
- 36. Ortiz, B. J.; Boursier, M. E.; Barrett, K. L.; Manson, D. E.; Amador-Noguez, D.; Abbott, N. L.; Blackwell, H. E.; Lynn, D. M. Liquid Crystal Emulsions That Intercept and Report on Bacterial Quorum Sensing. *ACS Appl. Mater. Interfaces* **2020**, *12*, 29056-29065.
- 37. Dan, A.; Agnihotri, P.; Brugnoni, M.; Siemes, E.; Wöll, D.; Crassous, J. J.; Richtering, W. Microgel-Stabilized Liquid Crystal Emulsions Enable an Analyte-Induced Ordering Transition. *Chem. Commun.* **2019**, *55*, 7255-7258.

- 38. Dan, A.; Aery, S.; Zhang, S.; Baker, D. L.; Gleeson, H. F.; Sarkar, A. Protein Microgel-Stabilized Pickering Liquid Crystal Emulsions Undergo Analyte-Triggered Configurational Transition. *Langmuir* **2020**, *36*, 10091-10102.
- 39. Pani, I.; K. M, F. N.; Sharma, M.; Pal, S. K. Probing Nanoscale Lipid-Protein Interactions at the Interface of Liquid Crystal Droplets. *Nano Lett.* **2021**, *21*, 4546-4553.
- 40. Tjipto, E.; Cadwell, K. D.; Quinn, J. F.; Johnston, A. P.; Abbott, N. L.; Caruso, F. Tailoring the Interfaces between Nematic Liquid Crystal Emulsions and Aqueous Phases via Layer-by-Layer Assembly. *Nano Lett.* **2006**, *6*, 2243-2248.
- 41. Gupta, J. K.; Sivakumar, S.; Caruso, F.; Abbott, N. L. Size-Dependent Ordering of Liquid Crystals Observed in Polymeric Capsules with Micrometer and Smaller Diameters. *Angew. Chem. Int. Ed.* **2009**, *48*, 1652-1655.
- 42. Kinsinger, M. I.; Buck, M. E.; Abbott, N. L.; Lynn, D. M. Immobilization of Polymer-Decorated Liquid Crystal Droplets on Chemically Tailored Surfaces. *Langmuir* **2010**, *26*, 10234-10242.
- 43. Zou, J.; Bera, T.; Davis, A. A.; Liang, W.; Fang, J. Director Configuration Transitions of Polyelectrolyte Coated Liquid-Crystal Droplets. *J. Phys. Chem. B* **2011**, *115*, 8970-8974.
- 44. Bera, T.; Fang, J. Polyelectrolyte-Coated Liquid Crystal Droplets for Detecting Charged Macromolecules. *J. Mater. Chem.* **2012**, *22*, 6807-6812.
- 45. Carlton, R. J.; Zayas-Gonzalez, Y. M.; Manna, U.; Lynn, D. M.; Abbott, N. L. Surfactant-Induced Ordering and Wetting Transitions of Droplets of Thermotropic Liquid Crystals "Caged" inside Partially Filled Polymeric Capsules. *Langmuir* **2014**, *30*, 14944-14953.
- 46. Guo, X.; Manna, U.; Abbott, N. L.; Lynn, D. M. Covalent Immobilization of Caged Liquid Crystal Microdroplets on Surfaces. *ACS Appl. Mater. Interfaces* **2015**, *7*, 26892-26903.
- 47. Verma, I.; Sidiq, S.; Pal, S. K. Poly (L-Lysine)-Coated Liquid Crystal Droplets for Sensitive Detection of DNA and Their Applications in Controlled Release of Drug Molecules. *ACS Omega* **2017**, *2*, 7936-7945.
- 48. Binks, B. P. Particles as Surfactants—Similarities and Differences. *Curr. Opin. Colloid Interface Sci* **2002**, *7*, 21-41.
- 49. Binks, B. P.; Rodrigues, J. A.; Frith, W. J. Synergistic Interaction in Emulsions Stabilized by a Mixture of Silica Nanoparticles and Cationic Surfactant. *Langmuir* **2007**, *23*, 3626-3636.
- 50. Cui, Z.-G.; Yang, L.-L.; Cui, Y.-Z.; Binks, B. Effects of Surfactant Structure on the Phase Inversion of Emulsions Stabilized by Mixtures of Silica Nanoparticles and Cationic Surfactant. *Langmuir* **2010**, *26*, 4717-4724.

- 51. Chevalier, Y.; Bolzinger, M.-A. Emulsions Stabilized with Solid Nanoparticles: Pickering Emulsions. *Colloids Surf. A Physicochem. Eng. Asp.* **2013**, *439*, 23-34.
- 52. Zhu, Y.; Jiang, J.; Liu, K.; Cui, Z.; Binks, B. P. Switchable Pickering Emulsions Stabilized by Silica Nanoparticles Hydrophobized in *situ* with a Conventional Cationic Surfactant. *Langmuir* **2015**, *31*, 3301-3307.
- 53. Wu, J.; Ma, G.-H. Recent Studies of Pickering Emulsions: Particles Make the Difference. *Small* **2016**, *12*, 4633-4648.
- 54. Binks, B. P. Colloidal Particles at a Range of Fluid–Fluid Interfaces. *Langmuir* **2017**, *33*, 6947-6963.
- 55. Ravera, F.; Ferrari, M.; Liggieri, L.; Loglio, G.; Santini, E.; Zanobini, A. Liquid-Liquid Interfacial Properties of Mixed Nanoparticle-Surfactant Systems. *Colloids Surf. A Physicochem. Eng. Asp.* **2008**, *323*, 99-108.
- 56. Binks, B. P.; Kirkland, M.; Rodrigues, J. A. Origin of Stabilisation of Aqueous Foams in Nanoparticle–Surfactant Mixtures. *Soft Matter* **2008**, *4*, 2373-2382.
- 57. Kirby, S. M.; Anna, S. L.; Walker, L. M. Effect of Surfactant Tail Length and Ionic Strength on the Interfacial Properties of Nanoparticle–Surfactant Complexes. *Soft Matter* **2018**, *14*, 112-123.
- 58. Whiteley, M.; Diggle, S. P.; Greenberg, E. P. Progress in and Promise of Bacterial Quorum Sensing Research *Nature* **2017**, *551*, 313-320.
- 59. Kowalczuk, P. B.; Drzymala, J. Physical Meaning of the Sauter Mean Diameter of Spherical Particulate Matter. *Part. Sci. Technol* **2016**, *34*, 645-647.
- 60. Maurya, N. K.; Mandal, A. Investigation of Synergistic Effect of Nanoparticle and Surfactant in Macro Emulsion Based Eor Application in Oil Reservoirs. *Chem. Eng. Res. Des.* **2018**, *132*, 370-384.
- 61. Wei, X.-Q.; Zhang, W.-J.; Lai, L.; Mei, P.; Wu, L.-M.; Wang, Y.-Q. Different Cationic Surfactants-Modified Silica Nanoparticles for Pickering Emulsions. *J. Mol. Liq.* **2019**, *291*, 111341.
- 62. Yekeen, N.; Padmanabhan, E.; Syed, A. H.; Sevoo, T.; Kanesen, K. Synergistic Influence of Nanoparticles and Surfactants on Interfacial Tension Reduction, Wettability Alteration and Stabilization of Oil-in-Water Emulsion. *J. Pet. Sci. Eng.* **2020**, *186*, 106779.
- 63. Briceño-Ahumada, Z.; Soltero-Martínez, J. F. A.; Castillo, R. Aqueous Foams and Emulsions Stabilized by Mixtures of Silica Nanoparticles and Surfactants: A State-of-the-Art Review. *Chemical Engineering Journal Advances* **2021**, *7*, 100116.

- 64. Atkin, R.; Craig, V. S.; Wanless, E. J.; Biggs, S. The Influence of Chain Length and Electrolyte on the Adsorption Kinetics of Cationic Surfactants at the Silica–Aqueous Solution Interface. *J. Colloid Interface Sci.* **2003**, *266*, 236-244.
- 65. Kume, G.; Gallotti, M.; Nunes, G. Review on Anionic/Cationic Surfactant Mixtures. *J. Surfact. Deterg.* **2008**, *11*, 1-11.
- 66. Tah, B.; Pal, P.; Mahato, M.; Talapatra, G. B. Aggregation Behavior of SDS/CTAB Catanionic Surfactant Mixture in Aqueous Solution and at the Air/Water Interface. *J. Phys. Chem. B* **2011**, *115*, 8493-8499.
- 67. Kumar, S.; Aswal, V. K.; Kohlbrecher, J. Size-Dependent Interaction of Silica Nanoparticles with Different Surfactants in Aqueous Solution. *Langmuir* **2012**, *28*, 9288-9297.
- 68. Zhu, Y.; Fu, T.; Liu, K.; Lin, Q.; Pei, X.; Jiang, J.; Cui, Z.; Binks, B. P. Thermoresponsive Pickering Emulsions Stabilized by Silica Nanoparticles in Combination with Alkyl Polyoxyethylene Ether Nonionic Surfactant. *Langmuir* **2017**, *33*, 5724–5733.

For Table of Contents Use Only:

